Journal of Hazardous Materials 307 (2016) 240–252

Contents lists available at ScienceDirect

Journal of Hazardous Materials

journal homepage: www.elsevier.com/locate/jhazmat

Development of a novel kinetic model for the analysis of PAH biodegradation in the presence of lead and cadmium co-contaminants.

Michael E. Deary[a,*], Chinedu C. Ekumankama[a], Stephen P. Cummings[b]

[a] Department of Geography,Faculty of Engineering and Environment, Northumbria University, Ellison Building, Newcastle upon Tyne NE1 8ST, United Kingdom
[b] Faculty of Health and Life Sciences, Northumbria University, Ellison Building, Newcastle upon Tyne NE1 8ST, United Kingdom

HIGHLIGHTS

- 40 week study of the biodegradation of 16 US EPA priority PAHs in a soil with high organic matter.
- Effects of cadmium, lead and mercury co-contaminants studied.
- Novel kinetic approach developed.
- Biodegradation of lower molecular weight PAHs relatively unaffected by Cd or Pb.
- Soil organic matter plays a key role in the PAH removal mechanism.

GRAPHICAL ABSTRACT

ARTICLE INFO

Article history:
Received 12 August 2015
Received in revised form
16 November 2015
Accepted 9 December 2015
Available online 11 December 2015

Keywords:
PAHs
Biodegradation
Kinetic modelling
Mercury
Cadmium
Lead
Co-contamination

ABSTRACT

We report on the results of a 40 week study in which the biodegradation of 16 US EPA polycyclic aromatic hydrocarbons (PAHs) was followed in microcosms containing soil of high organic carbon content (11%) in the presence and absence of lead and cadmium co-contaminants. The total spiked PAH concentration was 2166 mg/kg. Mercury amendment was also made to give an abiotic control.

A novel kinetic model has been developed to explain the observed biphasic nature of PAH degradation. The model assumes that PAHs are distributed across soil phases of varying degrees of bioaccessibility. The results of the analysis suggest that overall percentage PAH loss is dependent on the respective rates at which the PAHs (a) are biodegraded by soil microorganisms in pore water and bioaccessible soil phases and (b) migrate from bioaccessible to non-bioaccessible soil phases. In addition, migration of PAHs to non-bioaccessible and non-Soxhlet-extractable soil phases associated with the humin pores gives rise to an apparent removal process. The presence of metal co-contaminants shows a concentration dependent inhibition of the biological degradation processes that results in a reduction in overall degradation. Lead appears to have a marginally greater inhibitory effect than cadmium.

1. Introduction

Polycyclic aromatic hydrocarbons (PAHs) are ubiquitous compounds in the environment, arising mainly as a result of anthropogenic activities, particularly combustion or heat related processes involving hydrocarbons, such as coal gasification and waste incineration (pyrogenic origin) [1], though they may also be produced during natural processes, for example thermal geologic reactions and plant fossilisation (petrogenic origin) [2].

PAHs are both persistent and toxic, with several identified as carcinogens and mutagens [3]. They comprise two or more fused benzene rings and may also incorporate other ring structures as well as

* Corresponding author.
E-mail address: michael.deary@northumbria.ac.uk (M.E. Deary).

http://dx.doi.org/10.1016/j.jhazmat.2015.12.015

Table 1
Soil analysis results.

Category	Parameter	Value
Composition (%)	Clay	2.6
	Fine silt	4.5
	Medium silt	11.7
	Course silt	12.3
	Fine sand	48.7
	Medium sand	14.8
	Coarse sand	5.0
General soil properties	% Maximum water holding capacity	42.2 ± 1.7
	75% of maximum water holding capacity	31.7 ± 1.3
	% Nitrogen	0.37 ± 0.08
	% Organic carbon by elemental Analyser	11.00 ± 1.75
	Soil pH	6.02 ± 0.23
Potentially toxic elements (mg/kg ± 1 sd)	Cr	228 ± 45
	Ni	30 ± 2
	Cu	66 ± 6
	Zn	147 ± 8
	As	16 ± 3
	Se	<1
	Cd	<1
	Sn	16 ± 1
	Sb	11 ± 1
	Hg	<1
	Pb	201 ± 7

alkyl substituents. Those PAHs comprising entirely fused benzene rings, such as in naphthalene (2-ring) or phenanthrene (3-ring), are known as alternant PAHs whereas those incorporating other ring structures, such as in fluorene and and benzo[b]fluoranthene, are non-alternant. Table 1 summarises the structures of the USEPA priority list of 16 PAHs. These compounds, whilst important in terms of toxic potential and the mass fraction of PAHs they contribute in contaminated sites, represent only a fraction of the different PAH structural forms that can be found in such sites [4].

PAH-contaminated sites, particularly land associated with former gas works, can have total PAH concentrations ranging between a few hundred and several thousand mg/kg [5–7]. Biodegradation is the most common remediation method for PAH removal from soils and the literature has several good reviews of both practical applications [8–10] and underlying microbial mechanisms [1,11,12]. This process can be carried out by a wide variety of bacteria and filamentous fungi, with bacteria generally utilising the PAHs as carbon sources whereas fungal-based biodegradation is often part of a detoxification process [1]. Various other technologies for PAH remediation in soils have been reviewed in the literature [10] including: soil washing [13,14], electrochemical methods [15,16], chemical oxidation, including advanced oxidation processes [17,18], biochar application [19], ionising radiation treatment [20], thermal (microwave) treatment [21] and phytoremediation [22].

PAH structure has an important bearing on biodegradability, both from the perspective of the range of organisms that can metabolise specific PAHs, particularly those of higher molecular weight [23], but also through its influence on bioavailability and bioaccessibility (the subtleties of defining bioavailability and bioaccessibility in the context of contaminated soil have been deftly argued by Semple et al. [24]. In soil it has been observed that PAH degradation rates are inversely related to the number of rings in the structure [23], yet when biodegradation experiments are carried out in solution (two to four rings) this relationship does not hold [8]. These observations are likely to be due to reduced solution phase bioavailability of higher molecular weight PAHs that increasingly associate with the soil phase components [8]. In addition, PAHs may have limited bioaccessibility due to being physically or temporarily constrained from contact with the microorganisms, for example if they are located in within small pores, or are strongly adsorbed onto soil components [23]. Nevertheless some microorganisms, such as the ligninolytic fungi, *Phanerochaete chrysosporium*, *Berkandera adusta* and *Pleurotus ostreatus*, are able to grow directly on soil particles containing adsorbed PAHs, thus partially overcoming the effects of reduced bioavailability; moreover, they possess extracellular lignin peroxidise enzymes that can act directly upon the adsorbed phase. Indeed, the non-specificity of these enzymes means that they are able to metabolise a much greater range of PAH structural types than bacteria. Gramss et al. have shown that ligninolytic fungi significantly degrade 5–7-ring PAHs in soils, whereas limited biodegradation of these compounds takes place in the presence of bacteria alone [11]. Johnsen suggests that the limited number of bacteria that can grow on pure cultures of PAHs containing five or more aromatic rings is a consequence of low solution availability, and thus the restricted evolution of suitable enzymic pathways for their metabolism [23]. Some bacteria, such as species of *Nocardia*, *Pseudomonas* and *Mycobacterium* are also able grow directly on soil particles through the formation of biofilms [23] or to produce rhamnolipid biosurfactants that may solubilise the PAHs, thus increasing biodegradation rates [12,23]. Related to this, and affecting both the bioavailability and bioaccessibility of PAH's, is the process of 'soil ageing', whereby PAHs adsorbed onto the soil matrix migrate to increasingly inaccessible soil phases, ultimately to phases that are neither accessible to soil microorganisms nor extractable by robust methods such as Soxhlet [9]. A number of studies have shown that biodegradation is significantly inhibited in soils containing high levels of organic carbon, which has been ascribed to reduced bioavailability [9,25–29]. In effect, the soil is physically self-detoxifying, though this organic phase may ultimately degrade, releasing the previously unavailable PAHs. The implications of these processes from a regulatory perspective for persistent organic pollutants (POPs) are significant [30,31].

Soil environmental conditions will also have a significant influence on biodegradation rates. The original aim of this study was to investigate the effect of cadmium and lead co-contaminants on the biodegradation of the 16 US EPA priority list PAHs. This is important in terms of remediation potential of soils because industrial sites are often co-contaminated with potentially toxic elements [5,32].

However, in addition, the study has allowed us to develop a novel kinetic model that seeks to explain how the complex physical and biological processes occurring in soil determine the extent of biodegradation of PAHs of different structural types. Many studies have reported that PAH degradation in soil over extended periods can be described by biphasic kinetics, comprising an initial rapid phase over several days in which the PAHs are degraded by soil microorganisms followed by a slower phase over hundreds of days that reflects sequestering of the PAHs by soil organic matter during the soil ageing process [27,33,34]. Modelling approaches have been developed to reflect these different timescales; for example, over the short term, several models have utilised competitive inhibition enzyme kinetics to account for the availability of multiple PAH substrates in the solution phase [35–37] with some also including parameters to model the diffusion of PAH from soil to solution phase [35]. Other models, for example the Best equation, use a steady state approach to balance the diffusive and metabolic fluxes of substrates in solution [38–42]. More recently a number of compartmental models have been developed that take into account the rates of adorption/desorption from soil, sequestration into soil organic matter and Michaelis–Menton kinetics for biodegradation in solution [38,42]; these can be applied over the short and long term. Several models have also looked at the complex desorption phenomena alone over varying time periods [43–46]. Other modelling approaches have utilised multiple linear regression in which biodegradation extended periods (ca. 100 days) is related to soil organic carbon, humic and fulvic acid content and Log K_{ow} of the

PAH [47]. For soil biodegradation of POPs more generally, a number of compartmental models of varying complexity have been developed, the most successful of which take into account the soil ageing process [30]. In this paper, we describe a compartmental approach that takes into account movement of PAHs between three separate soil compartments, adsorption/desorption from soil to the aqueous phase and microbial degradation occurring in both the soil and aqueous phases.

2. Methodology

2.1. Overview

This was a 40 week soil microcosm study looking at the biodegradation of 16 USEPA priority list PAHs in the presence and absence of cadmium and lead co-contaminants at various concentrations. Soil used in the study was collected from Armstrong Park situated in the north–east of Newcastle upon Tyne, UK, approximately 2 km from the city centre (Grid Reference NZ 26626 65725). The specific location was a wooded greenfield site. Three significant lead works, all now decommissioned, were in operation within 3.5 km of the site and this has contributed to historically elevated lead levels in this area [48]. Approximately 200 kg of soil was collected from a layer extending down to 50 cm after removal of the surface vegetation.

The biodegradation experiments were carried out in microcosms cut from white PVC water piping (20 cm long and 3.2 cm diameter). Each soil treatment was divided into 39 separate microcosms, allowing replicates of three to be harvested for analysis at 1, 2, 3, 5, 7, 9, 12, 15, 20, 25, 30, 35 and 40 weeks. A sample was also taken immediately that the treatment had been made (0 weeks). Each microcosm contained 250 g of soil and was left open at the top but sealed with polythene at the bottom end. Microcosms were stored in a plant growth room at 20 °C with diurnal light cycle. Soil moisture was maintained at 75% of the maximum water holding capacity. The following treatments were set up: PAH only; PAH with target concentrations of 100, 250 and 500 mg/kg Cd; PAH with target concentrations of 100, 250 and 500 mg/kg Pb; abiotic control in which the PAH spiked soil was sterilised with a target concentration of 500 mg/kg mercury ($HgCl_2$), repeated at 7 weeks to maintain sterile conditions. PAH concentrations were determined by GC–MS analysis after extraction by accelerated solvent extraction (ASE).

2.2. Soil properties

Literature methods were used to determine soil pH [49], soil moisture [50] and soil water holding capacity [50]. Organic carbon and nitrogen content were determined on dried soil using a CE Instruments Flash 2000 elemental analyser. Particle size was determined using a Malvern Instruments Mastersizer S analyser [51].

Concentrations of potentially toxic elements in pelletised samples of soil were determined under vacuum by Energy Dispersive X-ray Fluorescence (EDXRF) using a Spectro Analytical X-Lab 2000 instrument operating a 5-target geology programme [52].

2.3. Soil spiking

In total, 91 kg of coal tar pitch spiked soil was required for the biodegradation experiments. Prior to spiking, the collected soil was homogenisised and air dried for 24 h before sieving to remove particles larger than 2 mm. The target concentration of total PAHs to be achieved from spiking was 2000 mg/kg. The appropriate mass of coal tar (Liver Grease, Oil and Chemical Co., Ltd., Liverpool, UK) required to achieve this concentration was dissolved in acetone as the carrier solvent. In total, 568 g powdered coal tar pitch (sieved to 2 mm) was dissolved in 9.1 L of acetone divided into four 2.5 L Winchester bottles; the coal tar pitch was allowed to dissolve over 48 h, during which time the bottles were regularly shaken. The solvent was applied to one quarter of the total required soil, i.e. 22.75 kg, in batches using a cement mixer. The spiked soil was allowed to air dry in a covered outside location and was then mixed with the remaining 68.25 kg soil in the cement mixer. By initially spiking only one quarter of the soil with acetone/coal tar pitch, any detrimental effects of the solvent on the soil microbial population were minimised. The coal tar pitch/solvent mixture was filtered through muslin prior to spiking so as to remove any undissolved solids.

Spiking with lead or cadmium at the required concentrations was achieved by dissolving the appropriate amount of either lead or cadmium chloride (analytical grade, Sigma–Aldrich) in the amount of distilled water required to bring the soil up to 75% of the maximum water holding capacity. The spiking procedure was carried out using a cement mixer. The same procedure was used to prepare a sterile abiotic control using $HgCl_2$.

2.4. PAH extraction and analysis

PAHs were extracted from soil microcosms using ASE (ASE 200 instrument, Dionex Ltd.) following the method of Lorenzi et al. [53] (Frost et al. have shown comparable extraction performance between Soxhlet and ASE for hexaconazole spiked onto soils for 0, 1 and 52 weeks [54]). Whole soil microcosms were harvested and the soil was dried, ground and passed through a 250 μm mesh sieve. The extraction was carried out on a 10 g sub-sample.

PAH analysis was carried on a Thermo Electron Corporation GC–MS fitted with a 30 m DB5 column using the calibration and quantification procedure developed in this laboratory by Lorenzi et al. [53]. A six-point calibration was carried out for each PAH (0–15 ppm) and R^2 values of at least 0.995 were obtained in each case, consistent with the results of Lorenzi et al. [53]. When applying the extraction and analysis procedure to a PAH-spiked soil reference standard (LGCQC3008-1), residual standard deviations for individual PAHs (RSDs) for triplicate measurements ranged between 6% (phenanthrene) and 24% (acenaphthylene) (mean = 14.8% for all 16 PAHs), with recoveries ranging between 73% (acenaphthene) and 105% (anthracene) (mean recovery = 93.4%, sd = 13.5). For the analysis of PAH spiked soil in the main investigation, a 10 ppm standard was run for every 10 samples and was used as part of the quantification process. For this study, a mean RSD for triplicate PAH determinations of 18.2% was obtained, with RSDs for individual PAHs as follows: naphthalene 15.7%; acenaphthylene, 25.9%; acenaphthene, 30.2%; fluorene, 26.3%; phenanthrene, 15.2%; anthracene. 17.2%; fluoranthene, 13.8%; pyrene, 11.9%; benzo[a]anthracene, 15.4%; chrysene, 14.7%; benzo[b]fluoranthene 17.0%; benzo[k]fluoranthene, 18.5%; benzo[a]pyrene, 16.8%; indeno[123-cd]pyrene, 15.9%; dibenzo[a,h]anthracene, 18.7% and benzo[g,h,i]perylene, 17.6%.

2.5. Development of the kinetic model

PAH degradation profiles in this study fitted reasonably well to a double exponential: it seems that the bulk effect of the complex physical and biological processes over significant time periods approximates to a sequential two step reaction, as described by Eq. (1). Here, PAH_{TE} is the concentration of total extractable PAHs, k_a and k_b are the rates for the two stepwise processes and Φ_a and Φ_b are the corresponding fractions of PAH_{TE} lost by each process.

$$[PAH_{TE}] = [PAH_{TE}]_0 \cdot \Phi_a \cdot e^{-k_a \cdot t} + [PAH_{TE}]_0 \cdot \Phi_b \cdot e^{-k_b \cdot t} \quad (1)$$

$$A \xrightarrow{k_a} B \xrightarrow{k_b} C$$

Scheme 1. Sequential two step reaction.

Kinetics that conform to a double exponential equation can have an underlying reaction scheme that is as simple as the two step process shown in Scheme 1 but can also be much more complex if the participating species are involved in equilibria and side reactions, as is likely to be the case for soil biodegradation processes.

From a consideration of the literature, we are likely to have a system, as defined in Scheme 2, that can be simplified to: (a) a soil moisture phase (PAH_{aq}), (b) a bioaccessible and extractable soil phase ($PAH_{B/E}$), (c) a non-bioacessible but ASE/Soxhlet-extractable soil phase ($PAH_{NB/E}$) and (d) a non-bioaccessible and non-ASE/Soxhlet-extractable soil phase ($PAH_{NB/NE}$) [8,11,12,23,24].

The two biological degradation processes are k_{bio}, which represents the soil moisture phase metabolism of PAHs, predominantly by bacteria, and k_{bio2}, which represents PAH degradation occurring on the soil phase, predominantly by fungi [11]. k_2 and k_3 represent physical processes associated with the transfer of PAHs into the different soil phases. The scheme assumes that the concentration of the enzymes responsible for the biotransformations (k_{bio} and k_{bio2}) are constant throughout the period during which the most of the biological activity takes place. Whilst it is likely that there will be a reduction of biomass with time as a result of stress due to the presence of PAHs and metal amendments, we will show that the biological degradation phase takes place relatively quickly, with the physical soil-phase transfer processes predominating at later times in the study.

Relating Scheme 2 to Scheme 1: $PAH_{B/E}$ and its associated equilibrium species equate to compartment A in Scheme 1, while $PAH_{NB/E}$ and $PAH_{NB/NE}$ equate to compartments B and C respectively.

An analytical solution to the system of differential equations arising from Scheme 2 will yield a double exponential equation of the general form shown in Eq. (1). In deriving such a solution we need to make a number of assumptions and simplifications. Firstly, it is likely that the forward and reverse reactions for the adsorption of PAH onto the soil matrix are rapid compared to the other processes and so we can write this as an equilibrium with the constant K, as in Eq. (2).

$$K = \frac{k_1}{k_{-1}} = \frac{[PAH_{B/E}]}{[PAH_{aq}]} \quad (2)$$

From Scheme 2 we can write separate rate laws for the loss of PAHs from the solution phase and from the bioaccessible soil phase as shown in Eqs. (3) and (4) respectively.

$$\frac{d[PAH_{aq}]}{dt} = -k_{bio} \cdot [PAH_{aq}] \quad (3)$$

$$\frac{d[PAH_{B/E}]}{dt} = -k_2 \cdot [PAH_{B/E}] - k_{bio2} \cdot [PAH_{B/E}] \quad (4)$$

We also need to define a mass balance for the total bioaccessible PAH, PAH_{TB}, in the soil and aqueous phases; this is shown in Eq. (5).

$$[PAH_{TB}] = [PAH_{aq}] + [PAH_{B/E}] \quad (5)$$

Making substitutions from Eqs. (2) and (5) we can re-write and combine Eqs. (3) and (4) in terms of $[PAH_{TB}]$, as shown in Eq. (5).

$$\frac{d[PAH_{TB}]}{dt} = -k_{bio} \cdot \left(\frac{[PAH_{TB}]}{K+1}\right) - k_2 \cdot \left(\frac{[PAH_{TB}] \cdot K}{K+1}\right) - k_{bio2} \cdot \left(\frac{[PAH_{TB}] \cdot K}{K+1}\right) \quad (5)$$

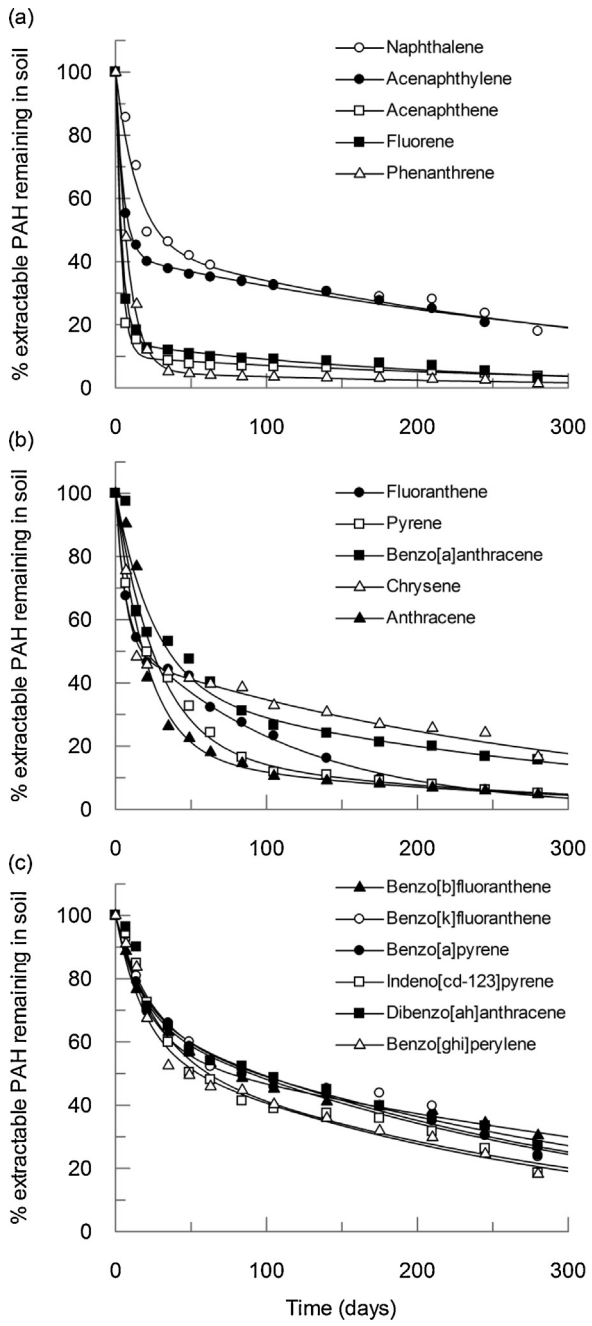

Fig. 1. Degradation of 16 PAHs in soil microcosms over a period of 280 days without added metals. The curves are the best fit to a double exponential (Eq. (1)) using the parameters listed in Table 2. All points are based on the average concentrations from three separate microcosms.

Furthermore, because the value of K is typically much greater than 1[1] we can make the additional assumption that $K + 1 \approx K$, thus allowing us to simplify Eqs. (5) to (6), i.e. the assumption is made that the PAHs are overwhelmingly in the bound form.

$$\frac{d[PAH_{TB}]}{dt} = -k_{bio} \cdot \left(\frac{[PAH_{TB}]}{K}\right) - k_2 \cdot [PAH_{TB}] - k_{bio2} \cdot [PAH_{TB}] \quad (6)$$

[1] For pyrene, K ranges from 71 to 1155 for soils ranging between 0.11 and 2.28% OC respectively so is likely to be considerably higher with the high OC contentof the soil used in this study (55. Means, J.C., et al., Sorption of polynuclear aromatic-hydrocarbons by sediments and soils. Environ. Sci. Technol., 1980. 14 (12): p. 1524–1528.).

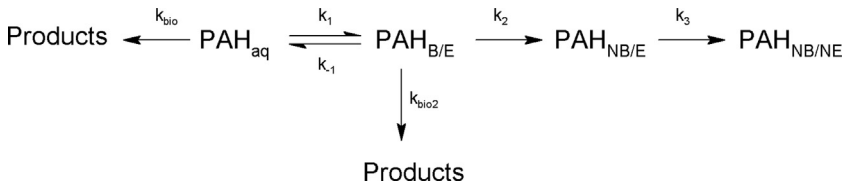

Scheme 2. Proposed scheme for transfer and degradation of PAHs in the soil environment.

Having defined the rate law for the bioaccessible fraction of the PAH, we now need to do the same for the non-bioaccessible but extractable PAH fraction, $PAH_{NB/E}$. This is described by Eq. (7), having substituted $[PAH_{TB}]$ for $[PAH_{B/E}]$ as per the derivation of Eq. (6) and having again making the simplifying assumption that $K+1 \approx K$.

$$\frac{d[PAH_{NB/E}]}{dt} = k_2 \cdot [PAH_{TB}] - k_3 \cdot [PAH_{NB/E}] \quad (7)$$

Finally, we need to consider the mass balance for the total extractable PAHs, PAH_{TE}, as defined by Eq. (8).

$$[PAH_{TE}] = [PAH_{TB}] + [PAH_{NB/E}] \quad (8)$$

An integrated rate equation can be obtained from Eqs. (6) and (7) by carrying out a Laplace transformation using Mathcad 15 and the approach of Korobov and Ochkov [56]. The procedure involves: (a) taking the Laplace transforms of Eqs. (6) and (7), (b) adding together the two transformed equations thus giving the total extractable PAH concentration, PAH_{TE} (as defined in Eq. (8)), and finally, (c) taking the inverse transform of the simplified form of the combined equation and rearranging to give the bi-exponential form shown in Eq. (9). It should be noted that $[PAH_{TB}]_0$ in Eq. (9) is equivalent to the total PAH concentration after initial spiking.

$$[PAH_{TE}] = [PAH_{TB}]_0 \cdot \frac{k_{bio} - K \cdot k_3 + K \cdot k_{bio2}}{k_{bio} + K \cdot k_2 - K \cdot k_3 + K \cdot k_{bio2}} \cdot e^{-\frac{(k_{bio}+K\cdot k_2+K\cdot k_{bio2})}{K}\cdot t} + [PAH_{TB}]_0 \cdot \frac{K \cdot k_2}{k_{bio}+K \cdot k_2 - K \cdot k_3+K \cdot k_{bio2}} \cdot e^{-k_3 \cdot t} \quad (9)$$

Comparing Eqs. (1) and (9), the pre-exponential rate and equilibria terms in Eq. (9) are equivalent to Φ_a and Φ_b in Eq. (1) and we can also see that k_a and k_b in Eq. (1) have the equivalences shown in Eqs. (10) and (11).

$$k_a = \frac{(k_{bio} + K \cdot k_2 + K \cdot k_{bio2})}{K} \quad (10)$$

$$k_b = k_3 \quad (11)$$

Thus k_a in Eq. (10) is a complex rate constant reflecting the equilibrium and various parallel reactions occurring for the bound and solution phase PAHs. k_b is equivalent to k_3, which is the rate for the abiotic transformation of the non bioaccessible but ASE/Soxhlet-extractable PAH, $PAH_{NB/E}$, to the non-extractable phase, $PAH_{NB/NE}$.

3. Results and discussion

3.1. Soil characteristics

The soil analysis results are shown in Table 1. Notable features are the high organic carbon content and the high background lead concentration. The latter is due to atmospheric emissions from historical lead works in the city and is not untypical for this area [48].

Table S1 in the Supplementary material shows the spiked metal concentrations for lead and cadmium at various stages during the 40 week study for both PAH amended and non-amended soils. The concentrations of metals in the soil generally decrease during the course of the study as a result of leaching following regular water addition to ensure constant soil moisture content. For the sterile microcosms, mercury chloride was added initially at a concentration of about 500 mg/kg Hg, with a further amendment at the same level required after 7 weeks because soil respiration and Ecoplate analysis (not shown) indicated some recovery in microbial activity after the first amendment.

3.2. Biodegradation in the absence of metal amendment

Biodegradation of organic substances in soil involves a complex community of bacteria and fungi with numerous enzymic pathways. In addition, the PAHs partition between the aqueous phase and multiple soil phases, each possessing a different degree of bioaccessibility. Despite such a complex environment, most literature PAH biodegradation studies report that PAH loss is described by either a single [9,29,57,58] or double [27,34,58] exponential equation. In the present study we also found the loss of extractable PAHs conformed to biphasic kinetics, as described by Eq. (1).

Table 2 summarises the calculated rate constants for these two processes for individual PAHs in the absence of metal amendment, together with the percentage of the reaction proceeding via the first step ($\Phi_a \times 100$); the corresponding kinetic profiles are shown in Fig. 1. All curve fitting analysis was carried out using the non-linear least squares method of Grafit version 7 [59]. It is interesting to note the range of different behaviours: acenanaphthene, fluorene and phenanthrene, degrade rapidly, dropping to below 10% of the starting concentration within 100 days, whereas naphthalene and acenanaphthylene drop to about 35% of the starting concentration in the same period before entering a slower removal phase.

A generalised biphasic kinetic model such as Eq. (1) provides no insight into the underlying physical and biological processes that account for the very different PAH degradation profiles that are observed across the range of PAH types in this study. However, our derivation of an equivalent form of this equation (Eq. (9)) that is based on the multi-compartment model described in Section 2.5, allows us to postulate an explanation for these profiles that is consistent with literature studies.

Further, if we assume in Eq. (9) that k_{bio} is small compared to the products $K\,k_{bio2}$ and $K\,k_2$ then Eq. (10) reduces to Eq. (12) and the corresponding pre-exponential term, Φ_a, reduces to Eq. (13). This is a reasonable assumption to make because (a) K, the soil/pore water equilibrium constant is likely to be in the hundreds or thousands [55], and (b) it is likely that as well as bacterial degradation of PAHs, which predominantly occurs in solution, we should also expect a large soil-based biodegradation component due to the significant fungal biomass that is likely to be present in these woodland originating soils [11].

$$k_a = k_2 + k_{bio2} \quad (12)$$

$$\Phi_a = 1 - \frac{k_2}{k_2 - k_3 + k_{bio2}} \quad (13)$$

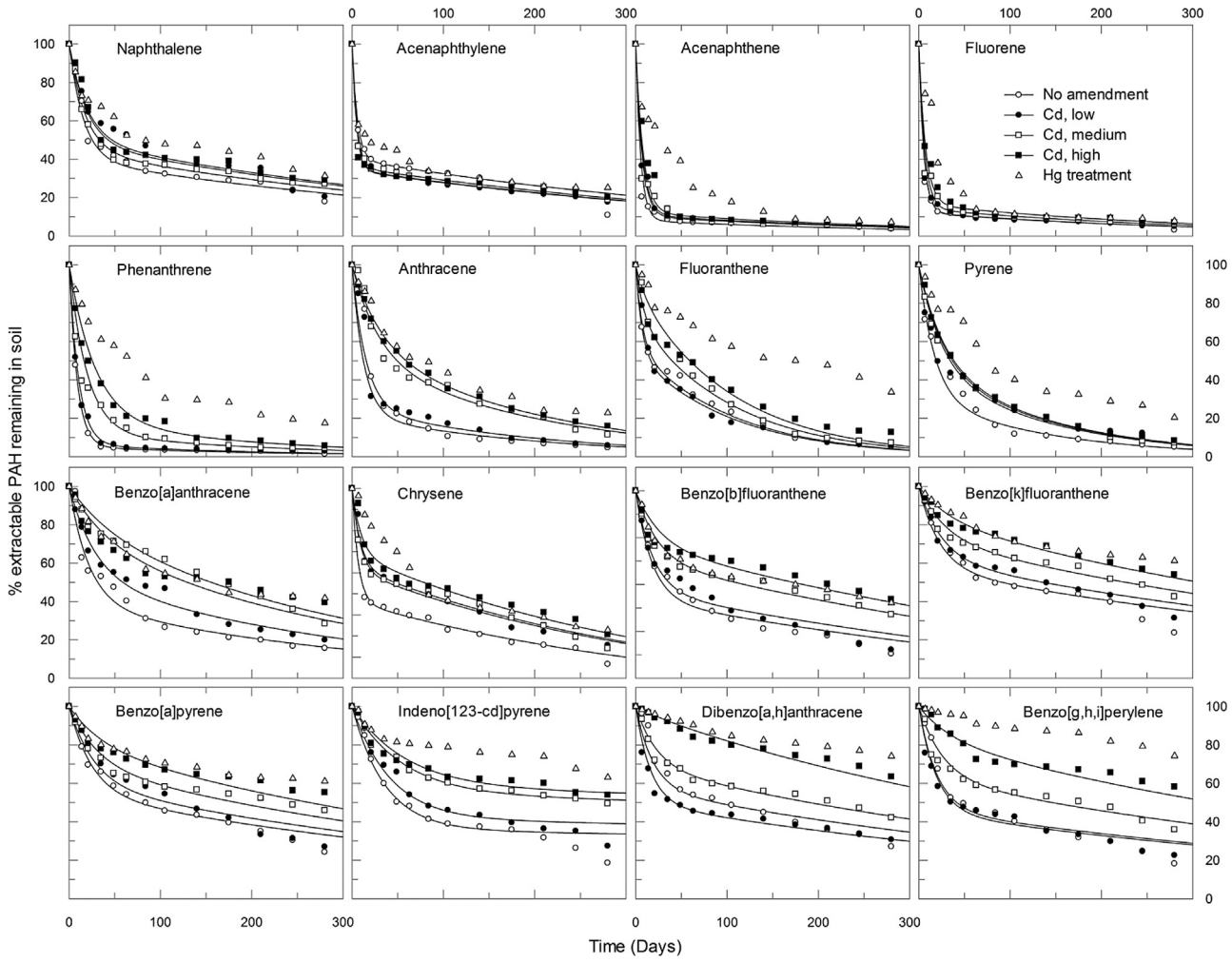

Fig. 2. Degradation of 16 PAHs in soil microcosms over a period of 280 days in the presence of cadmium at three concentrations. The curves are the best fit Eq. (14) using the parameters listed in Table 3. All points are based on the average concentrations from three separate microcosms. A mercury amended microcosm is included for comparison.

A consideration of Eq. (13) allows us to explain the range of kinetic profiles observed in Fig. 1. For the first step, k_a, the key relationship is that between k_{bio2}, the rate at which the PAHs are biodegraded, and k_2, the rate at which the bioaccessible PAH, $PAH_{B/E}$, migrates to the inaccessible yet extractable phase, $PAH_{NB/E}$. If $k_{bio2} > k_2$ then Φ_a, the fraction of the overall reaction proceeding via k_a, will approach 1, i.e. 100%. This is the case for acenanaphthene, fluorene and phenanthrene, where k_a is large, but also for anthracene and pyrene, where k_a is relatively small. However, in cases where k_{bio2} is equal to or lower than k_2 then Φ_a, will be 0.5 or lower, as we see for the majority of the high molecular weight PAHs where k_a is relatively low but also for naphthalene and acenanaphthylene where k_a is large.

In terms of how these rates relate to literature values, the rates for fluorene, anthracene and pyrene fall within the ranges listed in Maliszewska–Kordybach's review of such rates [29], though the value for chrysene observed in our study ($14.75 \times 10^{-2}\ d^{-1}$) is significantly higher than the fastest rate listed ($1.4 \times 10^{-2}\ d^{-1}$) for this PAH.

For the second step, k_b, we have shown that this equates to k_3, the migration of the bio-inaccessible but extractable PAH, $PAH_{NB/E}$, to the non-extractable fraction, $PAH_{NB/NE}$. Our values are consistent with those reported for the same process in sterile soil for pyrene and benzo[a]pyrene [9].

3.3. Refinement of the kinetic model and effect of metal amendment

Thus far our approach has been to calculate k_a, the value of the composite rate constant for the initial fast removal phase, from curve fitting analysis and to discuss the observed degradation profiles in terms of the likely ratios of the respective component biotic and abiotic rate constants, k_{bio2} and k_2. However the design of our overall study, employing non-amended and metal amended microcosms at three different concentrations for lead and cadmium allows for the determination of individual rate constants directly using a simplified form of Eq. (9), together with a global approach to curve fitting [60] that utilises kinetic data for studies at all metal amendment concentrations.

Applying the simplifications shown in Eqs. (12) and (13), Eq. (9) can be expressed in the form shown in Eq. (14). Of the three rate constants in Eq. (14), only k_{bio2} is likely to be significantly affected by the presence of metal co-contaminants; k_2 and k_3 relate to physical processes that should be largely unaffected by these changed conditions. Thus in the curve fitting procedure, k_2 and k_3 and can be set as global constants for all seven conditions for each PAH (control, plus three concentrations of each metal co-contaminant), with only k_{bio2} varying, allowing a robust determination of all three constants. This analysis was carried out using Grafit 7 with a global

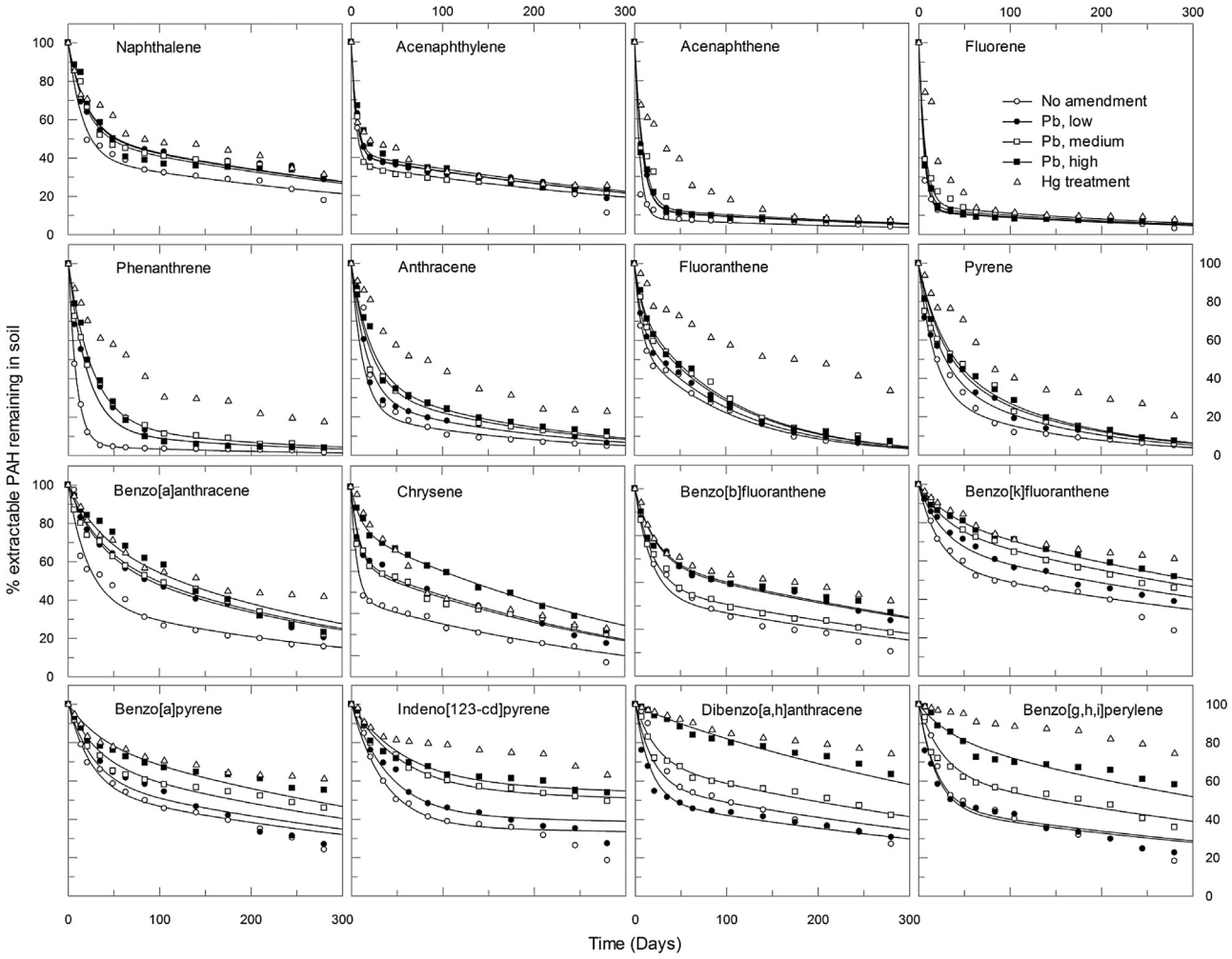

Fig. 3. Degradation of 16 PAHs in soil microcosms over a period of 280 days in the presence of lead at three concentrations. The curves are the best fit Eq. (14) using the parameters listed in Table 3. All points are based on the average concentrations from three separate microcosms. A mercury amended microcosm is included for comparison.

fit approach and proportional error weighting [60]. The results are shown in Table 3 , with corresponding plots shown in Figs. 2 and 3. Also shown in Table 3, is the parameter $\Phi_a \times 100$, the percentage loss of extractable PAH that occurs during the rapid initial phase, calculated from Eq. (13).

Generally the fits are very good across all PAHs and metal concentrations, indicating that the treatment of k_2 and k_3 as global constants is a reasonable one. Figs. 2 and 3 also include the profiles for PAH degradation in the presence of mercury, originally intended as a sterile control, though this eventually proved not to be possible because of the emergence of significant biological activity in these microcosms by week 7 (the microcosms were re-sterilised but it is likely that significant biodegradation had already taken place). Nevertheless, with few exceptions, loss of extractable PAHs is clearly much lower for the mercury amended samples.

$$[\mathrm{PAH_{TE}}] = [\mathrm{PAH_{TE}}]_0 \cdot 1 - \frac{k_2}{k_2 - k_3 + k_{\mathrm{bio2}}} \cdot e^{-(k_2 + k_{\mathrm{bio2}}) \cdot t} + [\mathrm{PAH_{TE}}]_0 \cdot \frac{k_2}{k_2 - k_3 + k_{\mathrm{bio2}}} \cdot e^{-k_3 \cdot t} \quad (14)$$

For microcosms without metal amendment, the calculated rate constants listed in Table 3 appear to show a dependence on PAH type, as demonstrated in Fig. 4 where they have been are plotted against Log K_{ow} of the PAH (similar patterns would have been obtained using RMM as the physical property). Most notably, in Fig. 4(a), k_3 values appear to show a Gaussian dependence on Log K_{ow}, with those for fluoranthene and pyrene, which are both compact 4-ring PAHs, located at the maxima of this distribution. This seems to indicate an optimum PAH size or binding affinity for the physical transfer of PAHs to the non-bioaccessible, non-bioavailable phase. For the other abiotic process, k_2, Fig. 4(b) shows that the rates are fairly consistent across the 16 PAHs, with the exception of acenaphthylene, fluoranthene and chyresene which all have rate constants some two to three times larger than the average for the others. Finally for k_{bio2}, with the exception of naphthalene and chrysene, there appears to be an inverse non-linear dependence on Log K_{ow}. This is consistent with literature observations that the range of soil microorganisms that can metabolise higher molecular weight PAHs is limited [23,11].

With regard to the effect of metal amendment on the k_{bio2} values in Table 3, generally there is a reduction in k_{bio2} as the metal concentration increases. Lead appears to have marginally greater inhibitory effect than cadmium, though it should be remembered that there was already a significant background lead concentration present in the soil before any spiking. There is also evidence from Table 3 that for some PAHs (acenaphthylene, fluoranthene and dibenzo[ah]anthracene) there is a slight stimulation in k_{bio2} compared to the control at low cadmium concentrations, which is consistent with some literature observations [61].

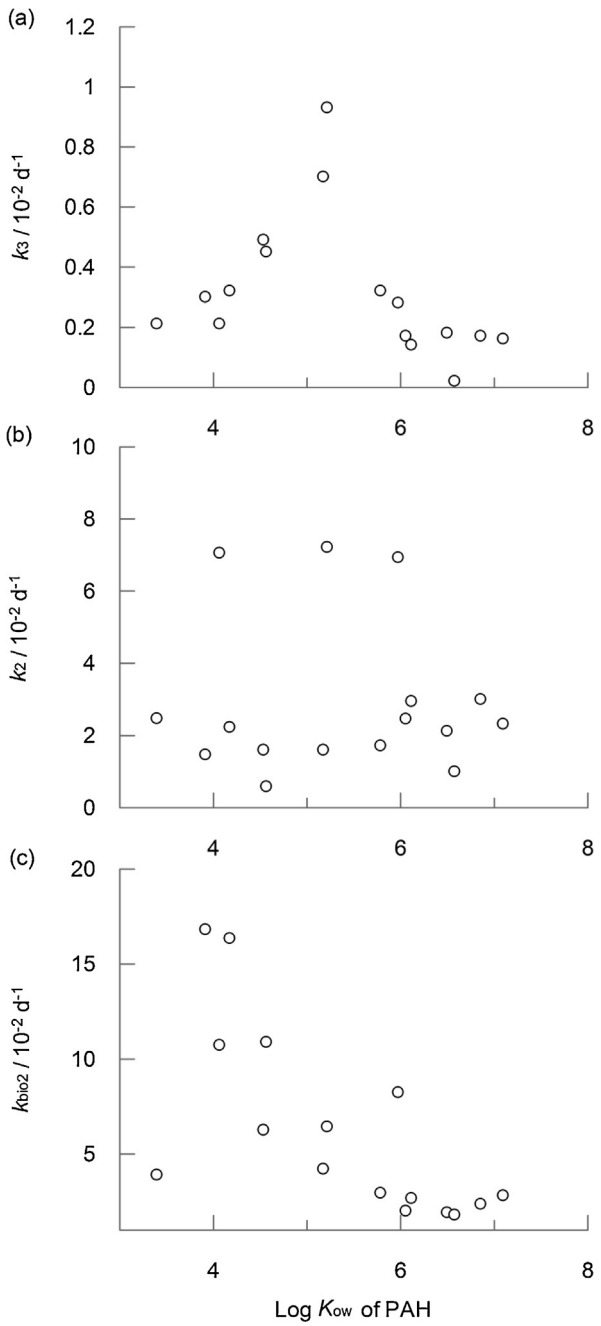

Fig. 4. Relationship between Log K_{ow} of PAHs and the respective biotic and abiotic rate constants listed in Table 3.

The influence of metals on microbial communities has been extensively reviewed by Baath [62] who notes a complex range of effects that are often difficult to fully elucidate because of the wide range of different investigative approaches used in literature studies. Overall, the relative order of toxicity is found to be Cd > Cu > Zn > Pb, which is at odds with the relative effects that we have observed, though there was significant variation within individual studies that were reviewed.

The most important effect of k_{bio2} inhibition as a result of metal amendment is the effect this has on Φ_a, the fraction of the overall PAH concentration that is removed as a result of biological activity, as defined by Eq. (13): the variation in the value of Φ_a in Table 3 reflects the changes in the ratio of k_{bio2} to k_2, as previously discussed. The overall effects of changes to this parameter as a result of metal amendment can be seen from Figs. 5 and 6 which show the percentage loss of extractable PAHs at 280 days for cadmium and lead respectively. Many of the lower molecular weight PAHs show only small reductions in overall degradation, even at the highest metal concentrations for the reasons discussed in Section 3.2. In contrast, higher molecular weight PAHs show marked reductions in overall degradation with increasing metal concentration.

3.4. Comparison with other modelling approaches

The model that we have developed has been shown to provide an explanation for the degradation profiles observed in soil for all 16 US EPA priority PAHs, with and without metal amendment. The analytical approach to solving the system of differential equations corresponding to our model has the advantage of clarity and transparency when determining the main factors responsible for the

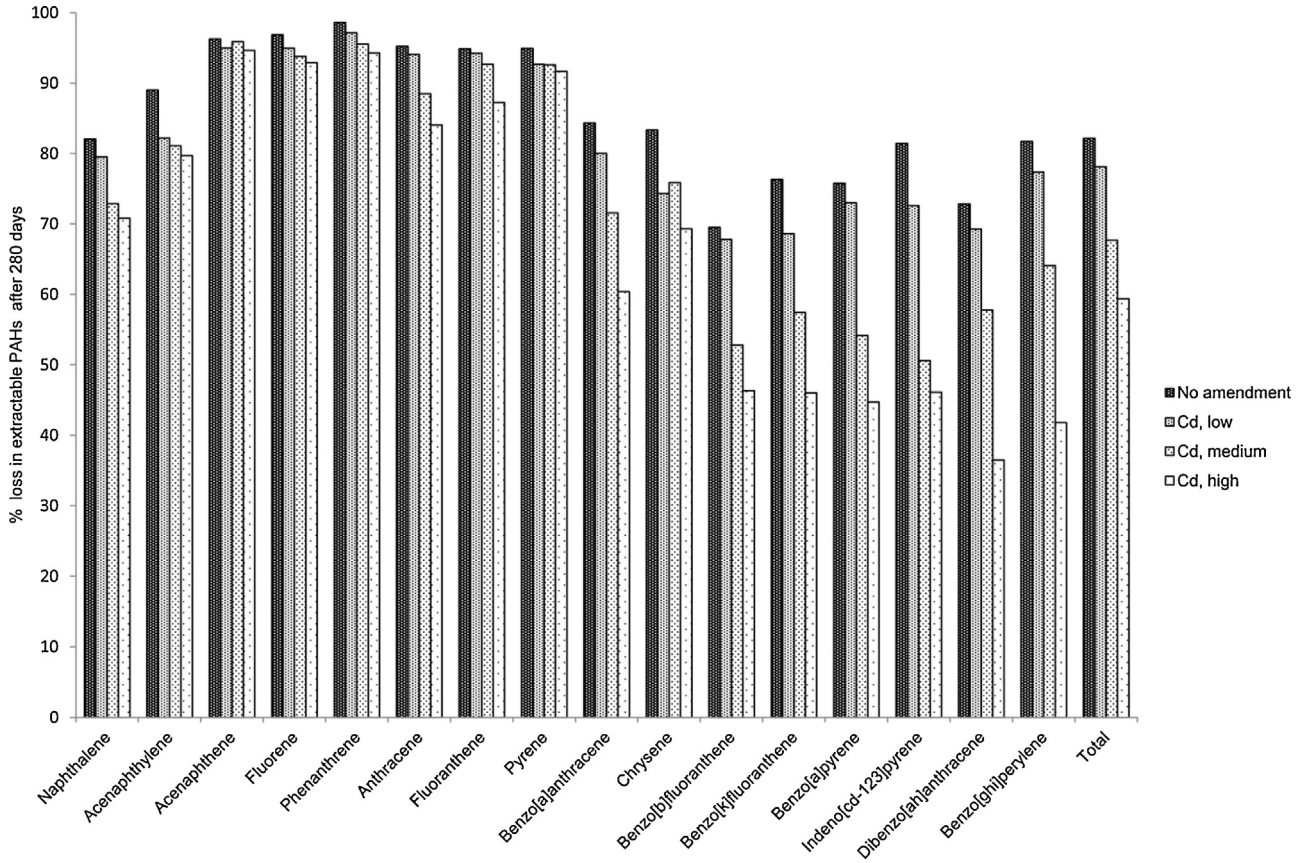

Fig. 5. Biodegradation of the 16 USEPA priority PAHs after 280 days in the presence of added cadmium.

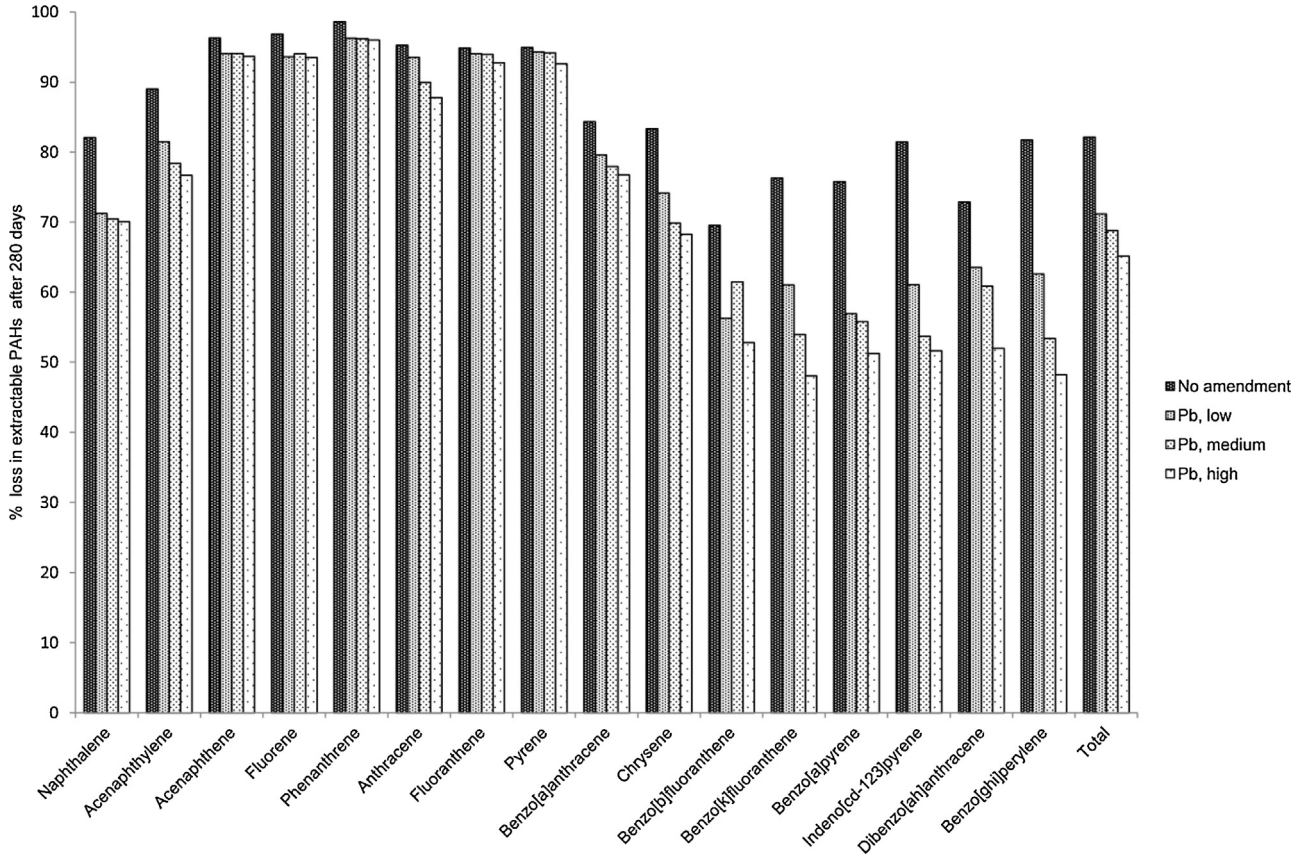

Fig. 6. Biodegradation of the 16 USEPA priority PAHs after 280 days in the presence of added lead.

Table 2
Initial concentrations and kinetic parameters for soil microcosm biodegradation studies shown in Fig. 1.

PAH	Structure	Initial concentration ± 1 σ (mg/kg)	$k_a/10^{-2}$ d^{-1}	$k_b/10^{-2}$ d^{-1}	% of reaction proceeding via k_a ($\Phi_a \times 100$)
Naphthalene		3.28 ± 0.63	6.92 ± 1.3	0.29 ± 0.04	54.7 ± 3.1
Acenaphthylene		1.44 ± 0.23	19.74 ± 1.84	0.26 ± 0.02	58.1 ± 0.9
Acenaphthene		7.75 ± 1.92	27.2 ± 2.75	0.32 ± 0.05	90.1 ± 0.7
Fluorene	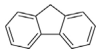	9.53 ± 1.63	24.39 ± 3.39	0.46 ± 0.05	85.7 ± 1.1
Phenanthrene		93.43 ± 15.08	12.06 ± 0.84	0.38 ± 0.06	94.8 ± 0.5
Anthracene	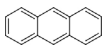	27.56 ± 4.12	4.87 ± 0.48	0.46 ± 0.07	82.4 ± 2.6
Fluoranthene	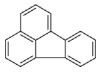	217.6 ± 35.6	19.02 ± 8.75	0.94 ± 0.04	40.9 ± 3.4
Pyrene		187.8 ± 31.5	3.68 ± 0.35	0.47 ± 0.08	80.7 ± 3.2
Benzo[a]anthracene	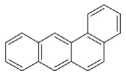	167.9 ± 25.9	3.93 ± 0.73	0.34 ± 0.06	61.1 ± 5.1
Chrysene	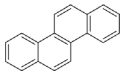	196.1 ± 33.3	14.75 ± 3.71	0.34 ± 0.03	51.3 ± 2.4
Benzo[b]fluoranthene	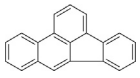	324.7 ± 55.5	4.81 ± 0.5	0.22 ± 0.02	42.3 ± 1.8
Benzo[k]fluoranthene	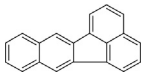	138.1 ± 20.1	6.05 ± 2.62	0.34 ± 0.04	31.1 ± 4.9
Benzo[a]pyrene	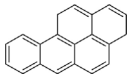	254.9 ± 40.12	5.75 ± 1.37	0.34 ± 0.02	32.6 ± 2.9
Indeno[123-cd]pyrene	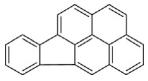	246.31 ± 43.1	4.3 ± 1.63	0.35 ± 0.05	42 ± 6.2
Dibenzo[a,h]anthracene	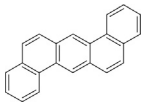	105.4 ± 17.9	4.72 ± 1.13	0.29 ± 0.03	34.7 ± 4.2
Benzo[g,h,i]perylene		184.5 ± 31.8	5.43 ± 1.79	0.38 ± 0.04	41.1 ± 4.2
Total	n/a	2166	8.58 ± 0.79	0.43 ± 0.01	40.6 ± 0.8

observed degradation profiles and in making the appropriate mathematical simplifications that allow the elucidation of individual rate constants.

There are many literature examples of modelling POP biodegradation using compartmental models, for example in the work of Adam et al. [38], Trapp and Rein [42] and Matthies et al. [30]; however our model has the advantage of incorporating the refinement of a non-bioaccessible but extractable soil phase ($PAH_{NB/E}$) in addition to the sequestered phase (equivalent to our $PAH_{NB/NE}$) that these other models employ. Our work has suggested that it is the ratio of the rates for PAH movement to this phase (k_2) and that for soil biodegradation (k_{bio2}) that is key to determining the overall extent of degradation. A further difference between our model and many of the literature models is that we have assumed a significant proportion, indeed the majority, of biodegradation to be occurring in the soil phase rather than in the solution phase. We have justified this on the basis of the high values of K, the equilibrium constant for PAH distribution in soil and aqueous phase [55], and the fact that the soil used in our study was obtained from a wooded area where there is likely to be significant fungal activity

Table 3
Fitting parameters for soil microcosm biodegradation studies.

PAH	Added metal	Added metal Conc.	$k_{bio2}/10^{-2}$ d^{-1}	$k_2/10^{-2}$ d^{-1}	$k_3/10^{-2}$ d^{-1}	$\Phi_a \times 100$ (% of removal occurring via first phase)
Naphthalene	None	–	3.89 ± 0.3	2.46 ± 0.28	0.21 ± 0.02	59.93 ± 0.50
	Cd	Low	2.79 ± 0.22			51.19 ± 0.45
		Medium	3.25 ± 0.25			55.27 ± 0.47
		High	2.65 ± 0.21			49.80 ± 0.45
	Pb	Low	2.46 ± 0.19			47.77 ± 0.44
		Medium	2.51 ± 0.2			48.32 ± 0.44
		High	2.65 ± 0.21			49.80 ± 0.45
Acenaphthylene	None	–	10.72 ± 0.57	7.05 ± 0.43	0.21 ± 0.01	59.85 ± 0.83
	Cd	Low	13.7 ± 0.72			65.68 ± 0.94
		Medium	12.7 ± 0.67			63.92 ± 0.90
		High	13.5 ± 0.7			65.34 ± 0.93
	Pb	Low	10.59 ± 0.57			59.55 ± 0.83
		Medium	12.7 ± 0.68			63.92 ± 0.91
		High	9.96 ± 0.54			58.04 ± 0.81
Acenaphthene	None	–	16.8 ± 0.98	1.46 ± 0.12	0.3 ± 0.04	91.87 ± 1.00
	Cd	Low	12.15 ± 0.77			89.03 ± 0.79
		Medium	13.01 ± 0.85			89.70 ± 0.87
		High	10.9 ± 0.76			87.89 ± 0.78
	Pb	Low	10.5 ± 0.69			87.48 ± 0.71
		Medium	9.62 ± 0.67			86.46 ± 0.69
		High	10.79 ± 0.71			87.78 ± 0.73
Fluorene	None	–	16.33 ± 0.76	2.22 ± 0.13	0.32 ± 0.03	87.82 ± 0.78
	Cd	Low	16.1 ± 0.78			87.67 ± 0.80
		Medium	13.57 ± 0.69			85.65 ± 0.71
		High	11.46 ± 0.61			83.38 ± 0.64
	Pb	Low	14.23 ± 0.7			86.24 ± 0.72
		Medium	12.57 ± 0.65			84.66 ± 0.68
		High	15.62 ± 0.79			87.33 ± 0.81
Phenanthrene	None	–	10.88 ± 0.57	0.58 ± 0.07	0.45 ± 0.06	94.73 ± 0.58
	Cd	Low	9.02 ± 0.47			93.66 ± 0.48
		Medium	4.51 ± 0.24			87.50 ± 0.27
		High	2.95 ± 0.15			81.17 ± 0.19
	Pb	Low	4.28 ± 0.25			86.85 ± 0.28
		Medium	3.3 ± 0.18			83.09 ± 0.21
		High	4.3 ± 0.25			86.91 ± 0.28
Anthracene	None	–	6.25 ± 0.53	1.59 ± 0.24	0.49 ± 0.05	78.37 ± 0.63
	Cd	Low	5.13 ± 0.39			74.48 ± 0.52
		Medium	1.9 ± 0.16			47.00 ± 0.38
		High	1.62 ± 0.14			41.54 ± 0.37
	Pb	Low	4.39 ± 0.34			71.04 ± 0.48
		Medium	3.38 ± 0.26			64.51 ± 0.43
		High	3.04 ± 0.23			61.59 ± 0.41
Fluoranthene	None	–	6.42 ± 0.85	7.21 ± 1.34	0.93 ± 0.02	43.23 ± 2.08
	Cd	Low	7.23 ± 0.99			46.63 ± 2.14
		Medium	3.73 ± 0.47			27.97 ± 1.95
		High	2.02 ± 0.26			13.13 ± 1.91
	Pb	Low	5.03 ± 0.65			36.25 ± 2.00
		Medium	3.29 ± 0.4			24.66 ± 1.94
		High	3.65 ± 0.46			27.39 ± 1.95
Pyrene	None	–	4.2 ± 0.34	1.59 ± 0.27	0.7 ± 0.05	68.76 ± 0.51
	Cd	Low	2.48 ± 0.16			52.82 ± 0.42
		Medium	2.33 ± 0.15			50.62 ± 0.41
		High	2.24 ± 0.14			49.20 ± 0.41
	Pb	Low	2.86 ± 0.2			57.60 ± 0.43
		Medium	2.32 ± 0.15			50.47 ± 0.41
		High	2.15 ± 0.14			47.70 ± 0.41
Benzo[a]anthracene	None	–	2.93 ± 0.28	1.71 ± 0.32	0.32 ± 0.03	60.42 ± 0.53
	Cd	Low	1.82 ± 0.15			46.73 ± 0.48
		Medium	0.71 ± 0.07			18.57 ± 0.46
		High	0.91 ± 0.08			25.65 ± 0.46
	Pb	Low	1.3 ± 0.1			36.43 ± 0.46
		Medium	1.22 ± 0.1			34.48 ± 0.46
		High	0.98 ± 0.08			27.85 ± 0.46
Chrysene	None	–	8.23 ± 0.61	6.92 ± 0.63	0.28 ± 0.01	53.46 ± 1.08
	Cd	Low	4.63 ± 0.34			38.60 ± 0.95
		Medium	4.35 ± 0.32			37.03 ± 0.95
		High	3.37 ± 0.25			30.87 ± 0.93
	Pb	Low	4.12 ± 0.3			35.69 ± 0.94
		Medium	4.35 ± 0.32			37.03 ± 0.95
		High	2.03 ± 0.17			20.18 ± 0.91

Table 3 (*Continued*)

PAH	Added metal	Added metal Conc.	$k_{bio2}/10^{-2}$ d^{-1}	$k_2/10^{-2}$ d^{-1}	$k_3/10^{-2}$ d^{-1}	$\Phi_a \times 100$ (% of removal occurring via first phase)
Benzo[b]fluoranthene	None	–	2.66 ± 0.18	2.94 ± 0.3	0.14 ± 0.02	46.15 ± 0.46
	Cd	Low	2.32 ± 0.15			42.58 ± 0.45
		Medium	1.36 ± 0.09			29.33 ± 0.43
		High	0.99 ± 0.07			22.43 ± 0.43
	Pb	Low	1.53 ± 0.1			32.10 ± 0.44
		Medium	2.27 ± 0.15			42.01 ± 0.45
		High	1.48 ± 0.1			31.31 ± 0.44
Benzo[k]fluoranthene	None	–	1.99 ± 0.12	2.45 ± 0.25	0.17 ± 0.01	42.62 ± 0.37
	Cd	Low	1.63 ± 0.09			37.34 ± 0.36
		Medium	1.07 ± 0.06			26.87 ± 0.36
		High	0.64 ± 0.04			16.10 ± 0.36
	Pb	Low	1.32 ± 0.07			31.94 ± 0.36
		Medium	0.88 ± 0.05			22.47 ± 0.36
		High	0.67 ± 0.04			16.95 ± 0.36
Benzo[a]pyrene	None	–	1.9 ± 0.17	2.11 ± 0.35	0.18 ± 0.02	44.91 ± 0.52
	Cd	Low	1.59 ± 0.14			40.06 ± 0.51
		Medium	1.1 ± 0.09			30.36 ± 0.50
		High	0.69 ± 0.06			19.47 ± 0.50
	Pb	Low	1.14 ± 0.09			31.27 ± 0.50
		Medium	0.98 ± 0.08			27.49 ± 0.50
		High	0.72 ± 0.06			20.38 ± 0.50
Indeno[123-cd]pyrene	None	–	1.79 ± 0.09	0.99 ± 0.14	0.02 ± 0.04	64.13 ± 0.22
	Cd	Low	1.41 ± 0.07			58.40 ± 0.21
		Medium	0.85 ± 0.04			45.60 ± 0.21
		High	0.73 ± 0.03			41.76 ± 0.20
	Pb	Low	1.05 ± 0.05			50.99 ± 0.21
		Medium	0.79 ± 0.03			43.75 ± 0.20
		High	0.98 ± 0.04			49.23 ± 0.21
Dibenzo[ah]anthracene	None	–	2.35 ± 0.16	2.99 ± 0.31	0.17 ± 0.02	42.17 ± 0.47
	Cd	Low	3.17 ± 0.22			50.08 ± 0.49
		Medium	1.5 ± 0.1			30.79 ± 0.45
		High	0.25 ± 0.06			2.61 ± 0.44
	Pb	Low	2.09 ± 0.14			39.10 ± 0.46
		Medium	1.45 ± 0.1			29.98 ± 0.45
		High	1.23 ± 0.09			26.17 ± 0.45
Benzo[g,h,i]perylene	None	–	2.8 ± 0.19	2.31 ± 0.26	0.16 ± 0.02	53.33 ± 0.41
	Cd	Low	2.95 ± 0.2			54.71 ± 0.42
		Medium	1.51 ± 0.1			36.89 ± 0.38
		High	0.6 ± 0.06			16.00 ± 0.37
	Pb	Low	1.54 ± 0.1			37.40 ± 0.38
		Medium	0.96 ± 0.07			25.72 ± 0.37
		High	0.8 ± 0.06			21.69 ± 0.37

and so a significant amount of biodegradation occuring on the soil phase [11].

4. Conclusion

A novel kinetic approach has been developed and successfully applied to the biexponential loss of extractable PAHs in soil, both in the presence and absence of metal co-contaminants. The results of our model suggest that the overall extent of biodegradation is dependent on respective rates at which the PAHs (a) are biodegraded by soil microorganisms in pore water and bioaccessible soil phases and (b) migrate from bioaccessible to non-bioaccessible phases. In addition, migration of PAHs to non-bioaccessible and non-Soxhlet-extractable phases associated with the humin pores gives rise to an apparent removal process. Our model suggests that two to four ring PAHs generally biodegrade at a much faster rate than they are transferred to the non-bioaccessible phase, whereas for five and six membered rings, these respective rates are more similar, leading to lower overall biodegradation.

The effect of metals on PAH degradation rates is varied, though generally there is an inhibitory effect that is dependent on concentration. Nevertheless, some stimulation of biodegradation is observed at low cadmium amendments for some PAHs, including for dibenzo[ah]anthracene. Lead appears to have marginally greater inhibitory effect than cadmium.

It is anticipated that the model will be applicable to soils with lower concentrations of organic matter, though for such environments the significance of the k_2 and k_3 processes should be less than for the current work.

Appendix A. Supplementary data

Supplementary data associated with this article can be found, in the online version, at http://dx.doi.org/10.1016/j.jhazmat.2015.12.015.

References

[1] C.E. Cerniglia, Biodegradation of pollycyclic aromatic hydrocarbons, Biodegradation 3 (1992) 351–368.
[2] C. Lors, et al., Evolution of bacterial community during bioremediation of PAHs in a coal tar contaminated soil, Chemosphere 81 (10) (2010) 1263–1271.
[3] W.M. Baird, L.A. Hooven, B. Mahadevan, Carcinogenic polycyclic aromatic hydrocarbon-DNA adducts and mechanism of action, Environ. Mol. Mutagen. 45 (2–3) (2005) 106–114.

[4] F. Haeseler, et al., Analytical characterization of contaminated soils from former manufactured gas plants, Environ. Sci. Technol. 33 (6) (1999) 825–830.
[5] P. Thavamani, M. Megharaj, R. Naidu, Bioremediation of high molecular weight polyaromatic hydrocarbons co-contaminated with metals in liquid and soil slurries by metal tolerant PAHs degrading bacterial consortium, Biodegradation 23 (6) (2012) 823–835.
[6] M. Eriksson, G. Dalhammar, A.K. Borg-Karlson, Biological degradation of selected hydrocarbons in an old PAH/creosote contaminated soil from a gas work site, Appl. Microbiol. Biot. 53 (5) (2000) 619–626.
[7] R.J.F. Bewley, P. Theile, D, in: K. Wolf, W.J. van den Brink, F.J. Colon (Eds.), Decontamination of a Coal Gasification Site through Application of Vangard Microorganisms, in Contaminated Soil, Kluwer Academic, Dordrecht, 1988, pp. 39–743.
[8] K.H. Wammer, C.A. Peters, Polycyclic aromatic hydrocarbon biodegradation rates: a structure-based study, Environ. Sci. Technol. 39 (8) (2005) 2571–2578.
[9] G.L. Northcott, K.C. Jones, Partitioning, extractability, and formation of nonextractable PAH residues in soil. 1. Compound differences in aging and sequestration, Environ. Sci. Technol. 35 (6) (2001) 1103–1110.
[10] S. Gan, E.V. Lau, H.K. Ng, Remediation of soils contaminated with polycyclic aromatic hydrocarbons (PAHs), J. Hazard. Mater. 172 (2–3) (2009) 532–549.
[11] G. Gramss, K.D. Voigt, B. Kirsche, Degradation of polycyclic aromatic hydrocarbons with three to seven aromatic rings by higher fungi in sterile and unsterile soils, Biodegradation 10 (1) (1999) 51–62.
[12] S. Hwang, Biodegradability of aged pyrene and phenanthrene in a natural soil, Chemosphere 47 (9) (2002) 891–899.
[13] E.V. Lau, et al., Extraction agents for the removal of polycyclic aromatic hydrocarbons (PAHs) from soil in soil washing technologies, Environ. Pollut. 184 (2014) 640–649.
[14] C.N. Mulligan, R.N. Yong, B.F. Gibbs, Surfactant-enhanced remediation of contaminated soil: a review, Eng. Geol. 60 (1–4) (2001) 371–380.
[15] A.T. Yeung, Y.Y. Gu, A review on techniques to enhance electrochemical remediation of contaminated soils, J. Hazard. Mater. 195 (2011) 11–29.
[16] M. Pazos, et al., Decontamination of soils containing PAHs by electroremediation: a review, J. Hazard. Mater. 177 (1–3) (2010) 1–11.
[17] V. Flotron, et al., Removal of sorbed polycyclic aromatic hydrocarbons from soil, sludge and sediment samples using the Fenton's reagent process, Chemosphere 59 (10) (2005) 1427–1437.
[18] F.J. Rivas, Polycyclic aromatic hydrocarbons sorbed on soils: a short review of chemical oxidation based treatments, J. Hazard. Mater. 138 (2) (2006) 234–251.
[19] D. Mohan, et al., Organic and inorganic contaminants removal from water with biochar, a renewable, low cost and sustainable adsorbent—a critical review, Bioresour. Technol. 160 (2014) 191–202.
[20] A.G. Chmielewski, Application of ionizing radiation to environment protection, Nukleonika 50 (2005) S17–S24.
[21] D.A. Jones, et al., Microwave heating applications in enviromnental engineering—a review, Resour. Conserv. Recy. 34 (2) (2002) 75–90.
[22] S.P. Pradhan, et al., Potential of phytoremediation for treatment of PAHs in soil at MGP sites, J. Soil Contam. 7 (4) (1998) 467–480.
[23] A.R. Johnsen, L.Y. Wick, H. Harms, Principles of microbial PAH-degradation in soil, Environ. Pollut. 133 (1) (2005) 71–84.
[24] K.T. Semple, et al., Defining bioavailability and bioaccessibility of contaminated soil and sediment is complicated, Environ. Sci. Technol. 38 (12) (2004) 228a–231a.
[25] W.D. Weissenfels, H.J. Klewer, J. Langhoff, Adsorption of polycyclic aromatic-hydrocarbons (Pahs) by soil particles—influence on biodegradability and biotoxicity, Appl. Microbiol. Biot. 36 (5) (1992) 689–696.
[26] A.J. Simpson, et al., Unraveling the structural components of soil humin by use of solution-state nuclear magnetic resonance spectroscopy, Environ. Sci. Technol. 41 (3) (2007) 876–883.
[27] K.J. Doick, et al., Long-term fate of polychlorinated biphenyls and polycyclic aromatic hydrocarbons in an agricultural soil, Environ. Sci. Technol. 39 (10) (2005) 3663–3670.
[28] N. Chung, M. Alexander, Effect of soil properties on bioavailability and extractability of phenanthrene and atrazine sequestered in soil, Chemosphere 48 (1) (2002) 109–115.
[29] B. Maliszewska-Kordybach, Dissipation of polycyclic aromatic hydrocarbons in freshly contaminated soils—the effect of soil physicochemical properties and aging, Water Air Soil Pollut. 168 (1-4) (2005) 113–128.
[30] M. Matthies, J. Witt, J. Klasmeier, Determination of soil biodegradation half-lives from simulation testing under aerobic laboratory conditions: a kinetic model approach, Environ. Pollut. 156 (1) (2008) 99–105.
[31] A. Craven, S. Hoy, Pesticide persistence and bound residues in soil—regulatory significance, Environ. Pollut. 133 (1) (2005) 5–9.
[32] H.I. Atagana, Biodegradation of polyacyclic aromatic hydrocarbons in contaminated soil by biostimulation and bioaugmentation in the presence of copper(II) ions, World J. Microb. Biot. 22 (11) (2006) 1145–1153.
[33] M.H. Huesemann, T.S. Hausmann, T.J. Fortman, Assessment of bioavailability limitations during slurry biodegradation of petroleum hydrocarbons in aged soils, Environ. Toxicol. Chem. 22 (12) (2003) 2853–2860.
[34] L. Luo, et al., Relationships between aging of PAHs and soil properties, Environ. Pollut. 170 (2012) 177–182.
[35] S.K. Lotfabad, M.R. Gray, Kinetics of biodegradation of mixtures of polycyclic aromatic hydrocarbons, Appl. Microbiol. Biotechnol. 60 (3) (2002) 361–366.
[36] M. Baboshin, L. Golovleva, Multisubstrate kinetics of PAH mixture biodegradation: analysis in the double-logarithmic plot, Biodegradation 22 (1) (2011) 13–23.
[37] C.D. Knightes, C.A. Peters, Multisubstrate biodegradation kinetics for binary and complex mixtures of polycyclic aromatic hydrocarbons, Environ. Toxicol. Chem. 25 (7) (2006) 1746–1756.
[38] I.K.U. Adam, et al., Experimental results and integrated modeling of bacterial growth on an insoluble hydrophobic substrate (phenanthrene), Environ. Sci. Technol. 48 (15) (2014) 8717–8726.
[39] T.N.P. Bosma, et al., Mass transfer limitation of biotransformation: quantifying bioavailability, Environ. Sci. Technol. 31 (1) (1997) 248–252.
[40] L.Y. Wick, T. Colangelo, H. Harms, Kinetics of mass transfer-limited bacterial growth on solid PAHs, Environ. Sci. Technol. 35 (2) (2001) 354–361.
[41] F. Volkering, et al., Microbial-degradation of polycyclic aromatic-hydrocarbons—effect of substrate availability on bacterial-growth kinetics, Appl. Microbiol. Biotechnol. 36 (4) (1992) 548–552.
[42] S. Trapp, A. Rein, Seventh framework programme: predictive model for PAH degradation and residue formation related to bioavailability, in molecular approaches and metagenomics investigations for clean-up of PAH contaminated sites European commission (2012).
[43] P. Mayer, et al., Enhanced diffusion of polycyclic aromatic hydrocarhons in artificial and natural aqueous solutions, Environ. Sci. Technol. 41 (17) (2007) 6148–6155.
[44] G. Marchal, et al., Impact of activated carbon, biochar and compost on the desorption and mineralization of phenanthrene in soil, Environ. Pollut. 181 (2013) 200–210.
[45] G. Marchal, et al., Comparing the desorption and biodegradation of low concentrations of phenanthrene sorbed to activated carbon, biochar and compost, Chemosphere 90 (6) (2013) 1767–1778.
[46] M.D. Johnson, T.M. Keinath, W.J. Weber, A distributed reactivity model for sorption by sails and sediments. 14. Characterization and modeling of phenanthrene desorption rates, Environ. Sci. Technol. 35 (8) (2001) 1688–1695.
[47] Y. Yang, et al., The effect of soil organic matter on fate of polycyclic aromatic hydrocarbons in soil: a microcosm study, Environ. Pollut. 158 (5) (2010) 1768–1774.
[48] A. Mellor, J.R. Bevan, Lead in the soils and stream sediments of an urban catchment in Tyneside, UK, Water Air Soil Pollut. 112 (3–4) (1999) 327–348.
[49] Y. Zhang, et al., Soil microbial characteristics under long-term heavy metal stress: a case study in Zhangshi wastewater irrigation area, Shenyang, Pedosphere 18 (1) (2008) 1–10.
[50] P. Vanhala, P. Tamminen, H. Fritze, Relationship between basal soil respiration rate, tree stand and soil characteristics in boreal forests, Environ. Monit. Assess. 101 (1–3) (2005) 85–92.
[51] M. Pansu, J. Gautheyrou, Handbook of Soil Analysis: Mineralogical, Organic and Inorganic Methods, Springer-Verlag, Heidelberg, 2007.
[52] J.R. Dean, et al., Characterisation and analysis pollutants and major: minor of persistent organic and trace elements in Calabash chalk, Chemosphere 57 (1) (2004) 21–25.
[53] D. Lorenzi, M. Cave, J.R. Dean, An inves tigation into the occurrence and distribution of polycyclic aromatic hydrocarbons in two soil size fractions at a former industrial site in NE England, UK using in situ PFE-GC–MS, Environ. Geochem. Health 32 (6) (2010) 553–565.
[54] S.P. Frost, et al., Extraction of hexaconazole from weathered soils: a comparison between soxhlet extraction, microwave-assisted extraction, supercritical fluid extraction and accelerated solvent extraction, Analyst 122 (9) (1997) 895–898.
[55] J.C. Means, et al., Sorption of polynuclear aromatic-hydrocarbons by sediments and soils, Environ. Sci. Technol. 14 (12) (1980) 1524–1528.
[56] V. Korobov, V. Ochkov, Chemical Kinetics with Mathcad and Maple, Springer-Verlag, New York, 2011.
[57] S. Maletic, et al., Degradation kinetics of an aged hydrocarbon-contaminated soil, Water Air Soil Pollut. 202 (1–4) (2009) 149–159.
[58] S. Thiele-Bruhn, G.W. Brummer, Kinetics of polycyclic aromatic hydrocarbon (PAH) degradation in long-term polluted soils during bioremediation, Plant Soil 275 (1–2) (2005) 31–42.
[59] R.J. Leatherbarrow, GraFit Version 7, Erithacus Software Ltd., Horley, U.K, 2009.
[60] M.E. Deary, S.M. Mousa, D.M. Davies, Effect of kosmotrope and chaotrope anions on rate and equilibria processes for the alpha-cyclodextrin catalysed reaction of 3-chloroperbenzoic acid with iodide, J. Incl. Phenom. Macro. 78 (1–4) (2014) 127–136.
[61] K.W. Wong, et al., Biodegradation of phenanthrene by the indigenous microbial biomass in a zinc amended soil, Lett. Appl. Microbiol. 40 (1) (2005) 50–55.
[62] E. Baath, Effects of heavy-metals in soil on microbial processes and populations (a review), Water Air Soil Pollut. 47 (3–4) (1989) 335–379.